CHAPTER 4

RESULTS AND DISCUSSION

4.1 Performance of Models in GVI Computation

With the 80 samples used for testing, the models are evaluated for their accuracy, robustness, and inference time. Table 4.1 records the evaluation results for each model.

Table 4.1 Evaluation of performances of different models for GVI computation.

Model	Mean Absolute Error (%)	Pearson Correlation Coefficient with true GVI (r)	5-95% of GVI Estimation Error	Inference time (seconds per 1000 data)
Pixel Segmentation model	6.7772	0.944534	(-0.065886, 0.198102)	9.99
DCNN end-to-end	4.5872	0.969098	(-0.067116, 0.087973)	43.87
DeepLabV3+ end-to-end	6.7139	0.924098	(-0.138696, 0.143834)	121.83

4.1.1 Accuracy Evaluation

According to the observations above, the DCNN end-to-end model have the highest accuracy out of the 3 models with the lowest mean absolute error at 4.58% and the highest Pearson correlation coefficient with the true GVI at 0.97 compared with that of 6.78%, 0.94 for the Pixel Segmentation model and 6.71%, 0.92, for the DeepLabV3+ model. Meanwhile, though DeepLabV3+ model has a slightly lower mean absolute error than the Pixel Segmentation model, it has a lower correlation coefficient with the true GVI compared with the Pixel Segmentation model. This shows that while DeepLabV3+ to be slightly worse off than the Pixel Segmentation method in capturing the patterns of the true GVI distribution.

4.1.2 Robustness Evaluation

The robustness of models is evaluated with 5-95% of GVI estimation error. In this case, the DCNN end-to-end model still shows the greatest performance with the smallest range of 5-95% GVI estimation error at 0.16 (-0.067116, 0.087973). This is much smaller than that of DeepLabV3+ and Pixel Segmentation models, with ranges of 0.28 (-0.138696, 0.143834) and 0.31 (-0.018923, 0.303153). The GVI estimation error is further explored with the charts in Figure 4.1 to understand the patterns of GVI prediction errors for each model. Constant line 0.075 is the mean absolute error of GVI for all 3 models while the other constant line in each chart is the mean absolute error for their respective models. X-axis is represented by grouped bins of GVI prediction with bin size of 0.05, while y-axis is represented by the mean absolute error of each bin.

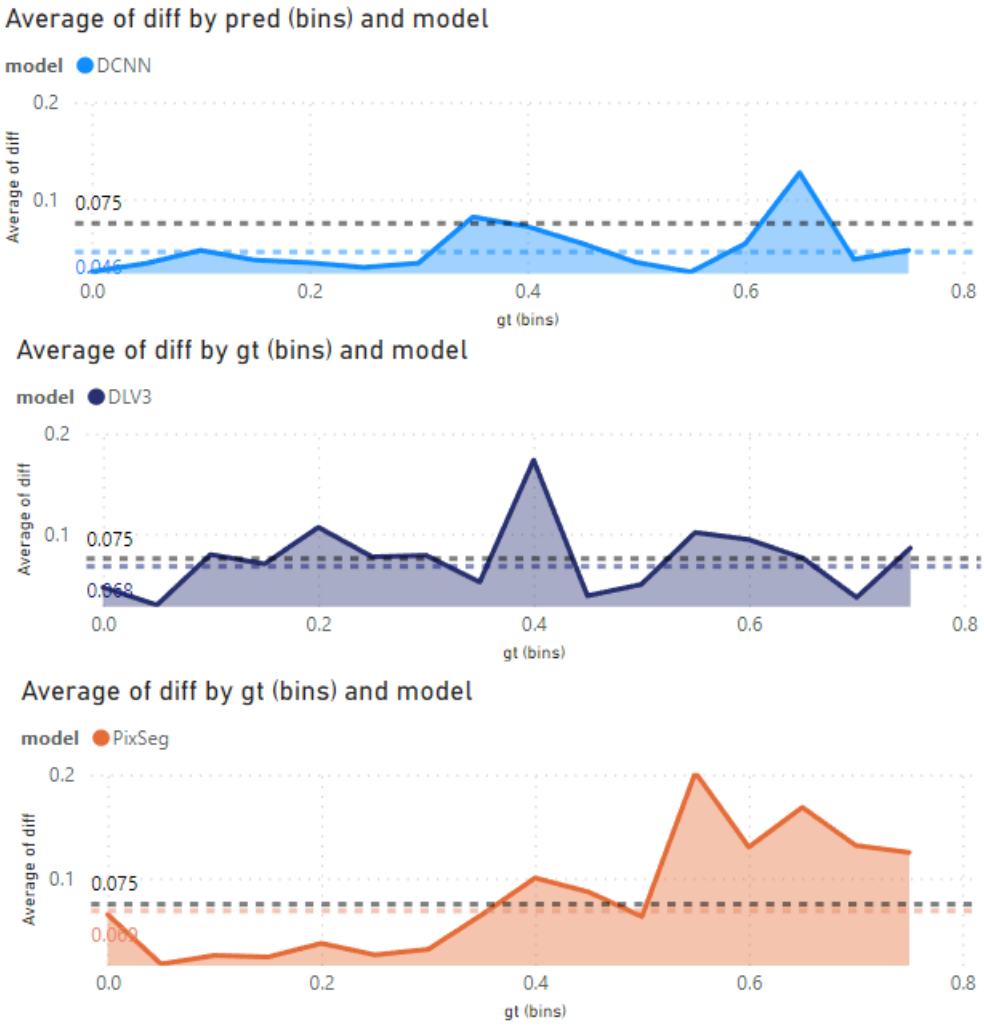

Figure 4.1 GVI prediction error for the 3 models studied.

In Figure 4.1, we can observe that the mean absolute error for DCNN predictions is consistently lower than the mean absolute error of all 3 models across various prediction bins. This is followed by the DeepLabV3+ model and the Pixel Segmentation model with similar mean absolute error at 0.068 and 0.069 respectively. Both have a different distribution where DLV3+ have the consistent error across prediction bins while Pixel Segmentation model has a very low error at lower predicted GVI but higher error with higher predicted GVI values.

4.1.3 Inference Time Evaluation

Unsurprisingly, the Pixel Segmentation model has the shortest inference time out of the 3 models with only 9.99s needed to predict 1000 GVI values due to the simplicity of its algorithm. It is followed by the DCNN model that can predict 1000 GVI values with 43.87s, and lastly DeepLabV3+ with 121.83s.

1.1.4 Bias Analysis for Prediction Models

The underlying bias of the models should be investigated to allow more interpretable prediction results for the users. In this case, the underlying bias of the models are studied by looking into how often the models underestimate and overestimate, and the distribution of the differences caused by it in Figure 4.2

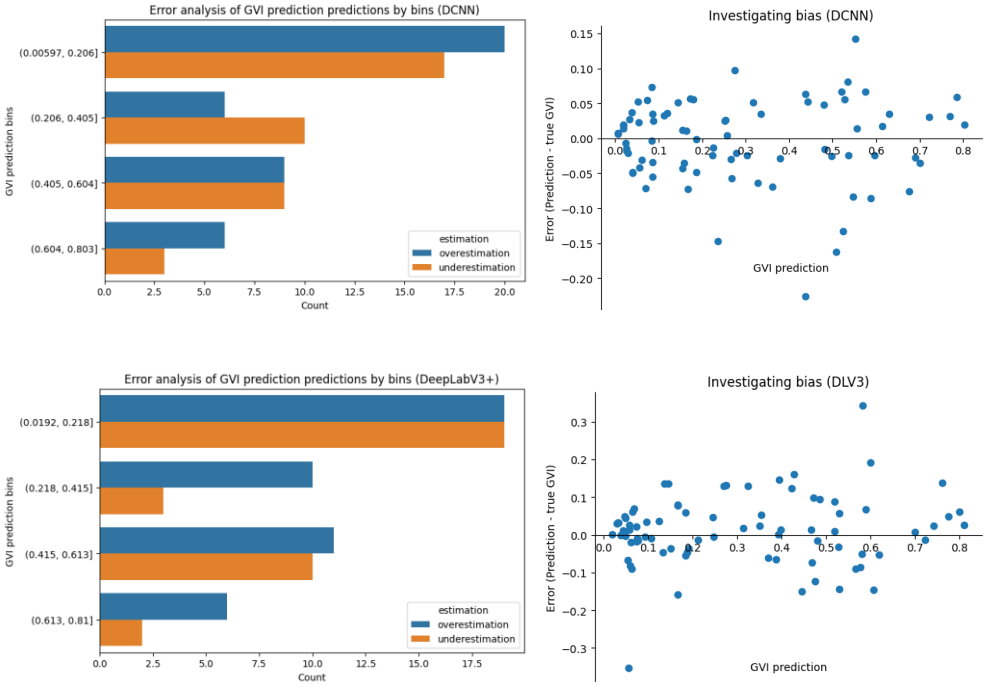

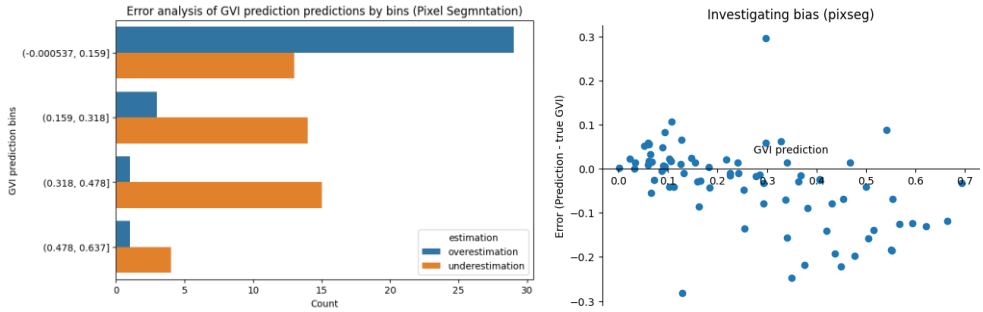

Figure 4.2 The frequency of underestimation and overestimation of model and bias investigation for 3 models.

In the charts above, it is observed that the DCNN model is relatively unbiased and DeepLabV3+ models are slightly positively biased by overestimating more than underestimating (46 vs 34). In the case of Pixel Segmentation model, it is negatively biased with 46 underestimations out of 80 testing data, with a very clear negative bias as shown in its error over GVI prediction chart.

1.2 Visualization of GVI Prediction in Study Site

Based on the model with higher accuracy, the predicted GVI values within the study site are visualized to allow further analysis on its urban vegetation coverage. In Figure 4.3, the mean GVI predictions at each one of the 1002 spots calculated by the mean GVI prediction at each single point where images are taken are visualized on a map plot. Red scatter plots represent spots with low GVI while green plots represent high GVI values. The distribution of predicted GVI are shown in the histogram on the right side of the dashboard, with purple dotted line representing its median and blue dotted line representing its mean.

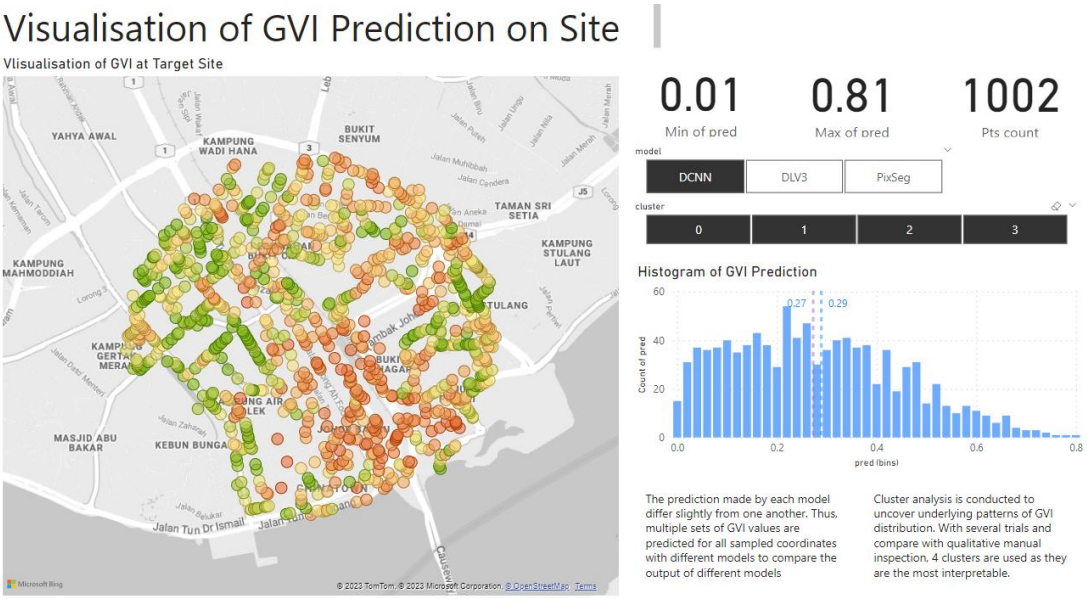

Figure 4.2 Dashboard visualising the GVI predictions on target site.

Based on Figure 4.1, there are several vague patterns discovered in the distribution of GVI values. For instance, the East side of the study site appears to have lower GVI values than the West; the South-East part of the site has the highest density of red points with low GVI. These observations suggest that GVI values in the study site vary due to their locations. To investigate the reasons contributing to the differences, clustering analysis is carried out in Chapter 4.4.

Due to the differences in each model the distribution of GVI predictions of 3 models are significantly different from one another. This can be observed from the histograms displayed in Figure 4.3.

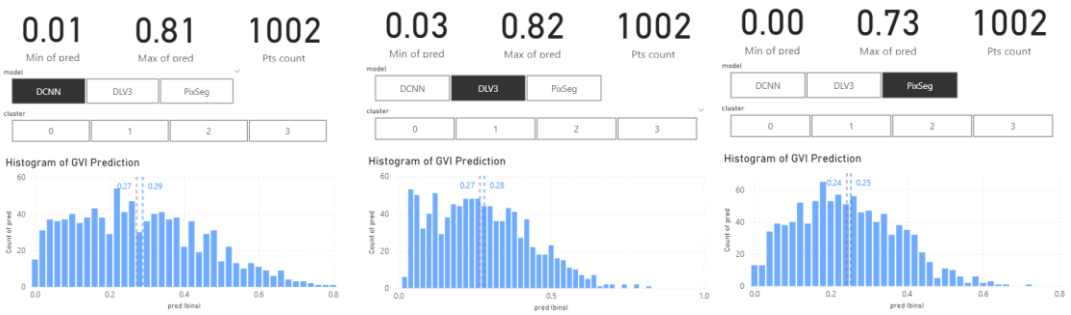

Figure 4.3 Distributions of GVI predictions with 3 different models.

For DCNN model, its GVI predictions have a unimodal, positive skew and a broad spread. It consists of a range from 0.01 to 0.81 for its predicted GVI. For SeepLavV3+

model, it has a unimodal, positive skew distribution for its GVI predictions. While it has a similar range with DCNN's prediction (0.03 to 0.82), its predictions have a slightly narrower spread compared with DCNN model's predictions.

As for the Pixel Segmentation model, it has a significantly more normal distribution compared with the other two as there is a shorter right tail. It has a smaller range of only 0.00 to 0.73.

1.3 Clustering Analysis of GVI

Both partition-based clustering and hierarchical clustering are carried out for all 3 models' GVI predictions (DCNN, DeepLavV3+, Pixel Segmentation) to determine the best clustering approach. As the location of sampling is an important part of the analysis, the latitude and longitude of sample points are included in the clustering analysis as well.

For partition-based clustering (Kmeans) and hierarchical clustering (agglomerative clustering), the number of clusters needs to be predetermined based on the insights that we are extracting and how well one cluster differentiates from another. In this project, the latter is informed by utilizing silhouette score. Therefore, in Figure 4.4 and 4.5, silhouette score is plotted against the number of clusters for both clustering approaches applied on different models' predictions.

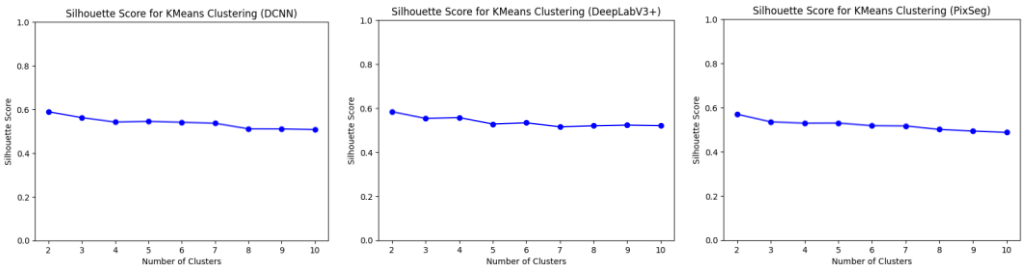

Figure 4.4 Kmeans clustering for GVI predictions based on DCNN, DeepLabV3+ and Pixel Segmentation model.

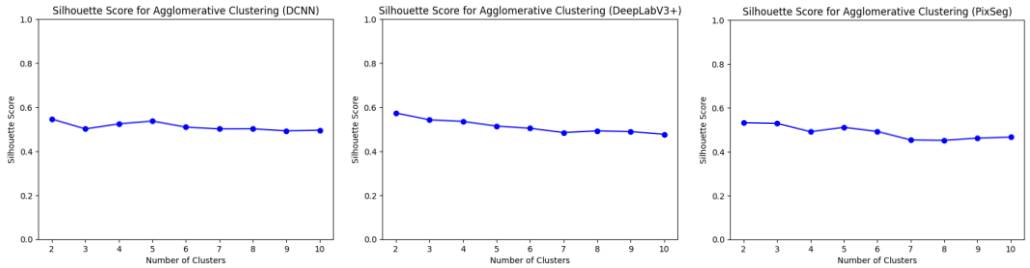

Figure 4.5 Agglomerative clustering for GVI predictions based on DCNN, DeepLabV3+ and Pixel Segmentation model.

In Figure 4.4 and Figure 4.5, we also notice that Kmeans has a slightly higher silhouette score compared to that of agglomerative clustering across all number of clusters tested. Thus, Kmeans is selected as the method for clustering analysis. To ensure that Kmeans is suitable for the dataset, latitude, longitude and mean GVI prediction per sample spot is plotted in a 3D scatterplot to ensure the data distribution is spherical in Figure 4.6.

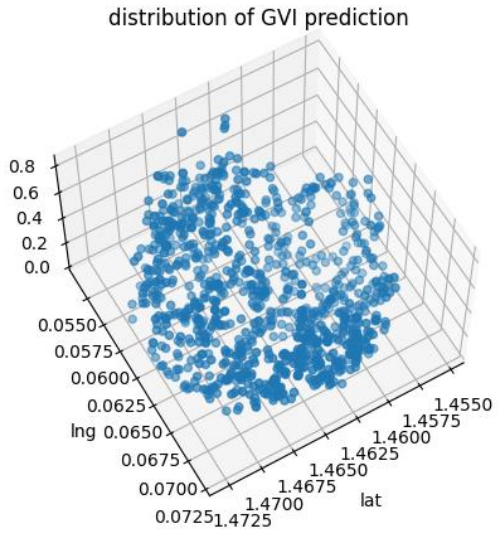

Figure 4.6 Scatterplot latitude, longitude, mean GVI predictions on 3D-space to see if the data distribution is spherical.

As silhouette score remains similar with different number of clusters as shown in Figure 4.4 and Figure 4.5, elbow method is used to determine the number of clusters for Kmeans clustering. The inertia of clusters are plotted against the number of clusters in Figure 4.7 where the inflection point (‘elbow’) is chosen to be the number of clusters. In this case, the number of clusters is chosen to be 4.

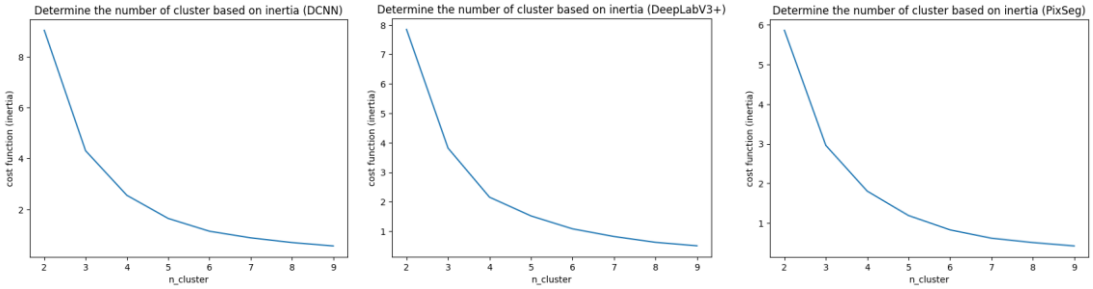

Figure 4.7 Determine the number of clusters with elbow method.

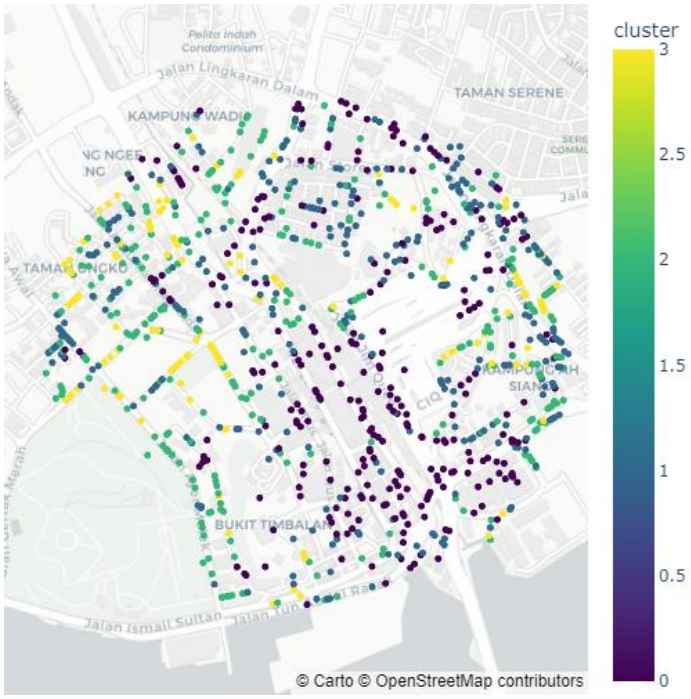

Figure 4.8 Visualization of hierarchical clusters (DCNN, cluster=4).

Figure 4.8 shows an example of clustering results based on DCNN GVI predictions and location of sampling points visualised on map. As DCNN has the best performance in terms of accuracy, robustness and biasness, only its predictions are used for further clustering analysis in the following sections.

In the following section, the characteristics of each cluster are explored and analyzed in detail.

1.3.1 Cluster 0

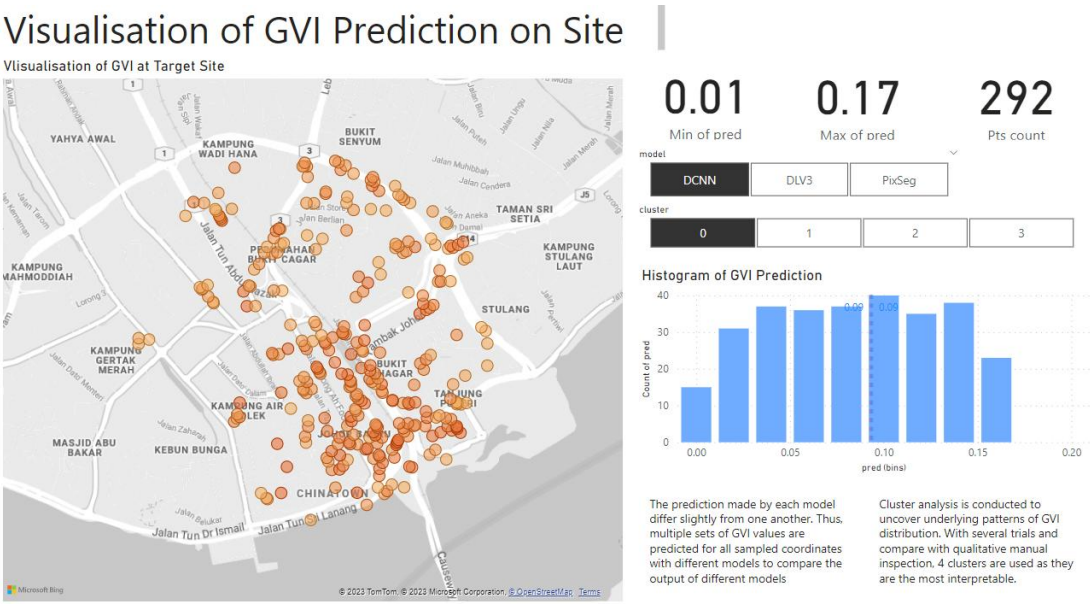

Figure 4.9 Visualization of cluster 0 for DCNN Kmeans clustering.

Cluster 0 has the lowest predicted GVI values. There are 292 spots where GVI is in the lowest range of 0.01 and 0.17. Their average and median GVI are as low as 0.09. From the map plot, we can observe that there are certain characteristics to where these low GVI spots are located.

For instance, they are often located on highways and main roads without any observable vegetation. Figure 4.10 highlights the vehicular roads where spots with low predicted GVI values from cluster 0 are located and Figure 4.11 illustrates sample GSV taken from these locations.

Figure 4.10 Roads that intersect with or adjacent to spots from cluster 0.

From Figure 4.10, we can notice that there are very few ……. While it is a lot harder to plant trees in these areas due to maintenance and arrangements issues, the presence of a lot of such spots can represent a problem in urban design as it creates too much very uncomfortable space for its users.

Figure 4.11 Sample GSV images taken from highways and main roads with very little observable vegetation.

While it is a lot harder to plant trees in these areas due to maintenance and arrangements issues, the presence of a lot of such spots can represent a problem in urban design as it creates too much very uncomfortable space for its users.

Other than highways and large vehicular roads, there are also certain zones, especially at the Southern part of the site with dense commercial zones as shown in Figure 4.12, with sample GSV images illustrated in Figure 4.13. Due to the high density of these areas and the lack of green space planning, these places have very low GVI in result.

Figure 4.12 Highlights on the city center with high density commercial area.

Figure 4.13 Sample GSV images taken from areas highlighted in Figure 4.12.

In conclusion, in Cluster 0, we can notice plenty urban spaces in the target site with very low predicted GVI values, with a lot of them on main road or highway and the densely populated commercial zone at the Southern part of the Johor Bahru city center. This illustrate possible fundamental flaws in the vehicle-centric and careless urban planning for the Johor Bahru city center without consideration for green spaces.

4.3.2 Cluster 1

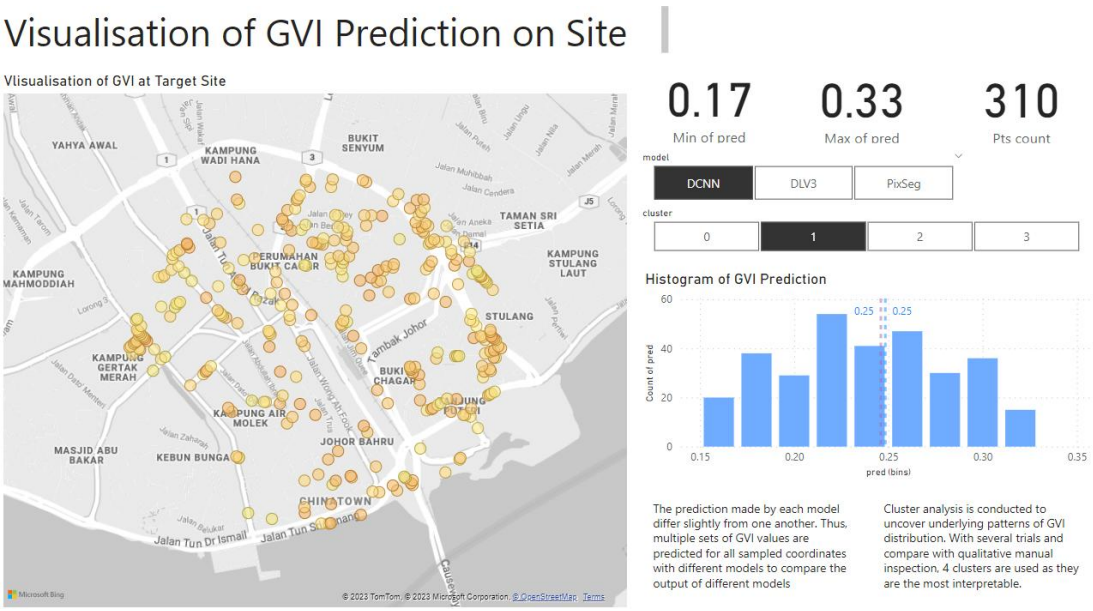

Figure 4.14 Visualization of cluster 1 for DCNN Kmeans clustering.

Cluster 1 has higher predicted GVI values than Cluster 0. There are 310 spots where GVI is in the lower range of 0.17 and 0.33. Their average and median GVI are both 0.25. From the map plot, we can observe Cluster 1 is much more evenly scattered compared with Cluster 0. This shows that the GVI values in Cluster 1 is more commonly experienced in the Johor Bahru City Center.

In fact, by inspecting the GSV images in Cluster 1, we can observe that the spots in Cluster 1 are mostly in active commercial and residential areas that makes up a very big part of our experience in a place. In Figure 4.16 and Figure 4.17, GSV from commercial areas and residential marked in Figure 4.15 are illustrated respectively.

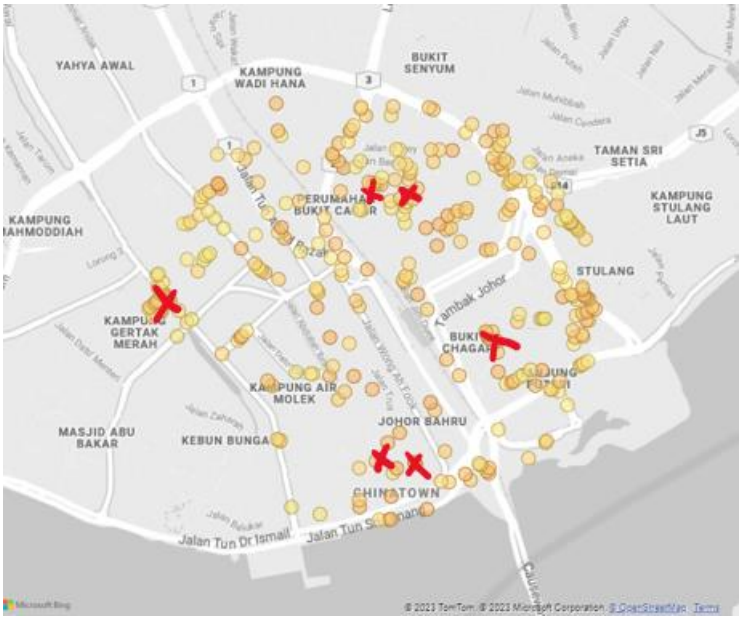

Figure 4.15 Indication of the sampling location for GSV images displayed in Figure 4.16 and Figure 4.17.

Figure 4.16 Sample GSV images from commercial areas marked in Figure 4.15.

Figure 4.17 Sample GSV images from residential areas marked in Figure 4.15.

In conclusion, we can notice sampling spots from Cluster 1 scattering evenly across the Johor Bahru city center, especially active commercial and residential areas, forming a major part of the experience of the urban space users. In these places with GVI in the range of 0.17 and 0.33, there are plenty of green views compared with the spots in Cluster 0 with green belts, street trees, etc.

4.3.3 Cluster 2

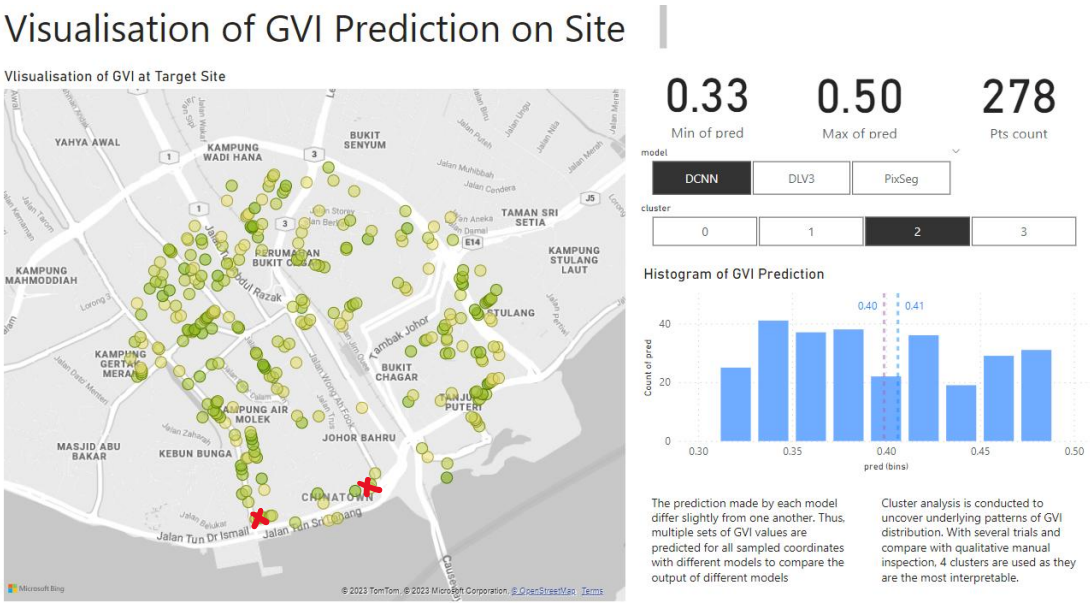

Figure 4.18 Visualization of Cluster 2 for DCNN Kmeans clustering.

Cluster 2 has the second highest predicted GVI values. There are 278 spots where GVI is in the higher range of 0.33 and 0.50. Their average and median GVI are 0.41 and 0.40 respectively. From the map plot, we can observe Cluster 2 is much more focused at the North, East and West part of the site.

By visualizing the aerial view of the plot, we can realize that this is the case as the distribution of Cluster 3 points are usually located adjacent to the green pocket spaces or belts in the city center. Due to the high density of man-made structures and buildings at the Southern side, it is harder to incorporate these spaces at the Southern side. Figure 4.19

displays the aerial view and grayscale map where Cluster 3 points are plotted on to illustrate the observation mentioned above.

Figure 4.19 displays the aerial view and grayscale map where Cluster 3 points are plotted on.

Compared with large scale parks or forests, these small green areas are more effective in permeating the city and can introduce green views to the daily to more places. Figure 4.21 illustrates GSV of places where these green pocket spaces increase the predicted GVI of the spot. Indication of where images in Figure 4.21 are sampled from is displayed in map-plot in Figure 4.20.

Figure 4.20 Indication of the sampling location for GSV images displayed in Figure 4.21.

Figure 4.21 Sample GSV images marked in Figure 4.20.

Last but not least, there is an interesting observation in the Chinatown street located at the densest commercial area, i.e. despite the small street, they managed to incorporate small street trees, thereby significantly increase the predicted GVI values on the street. This shows that the dense commercial areas in Cluster 0 have the potential to increase their GVI with more street trees despite the lack of space. In Figure 4.22, GSV image of the street incorporating street trees in the walkway on the Chinatown street.

Figure 4.22 GSV image of the street incorporating street trees in the walkway on the Chinatown street. Its location is marked on the map on the left.

4.3.4 Cluster 3

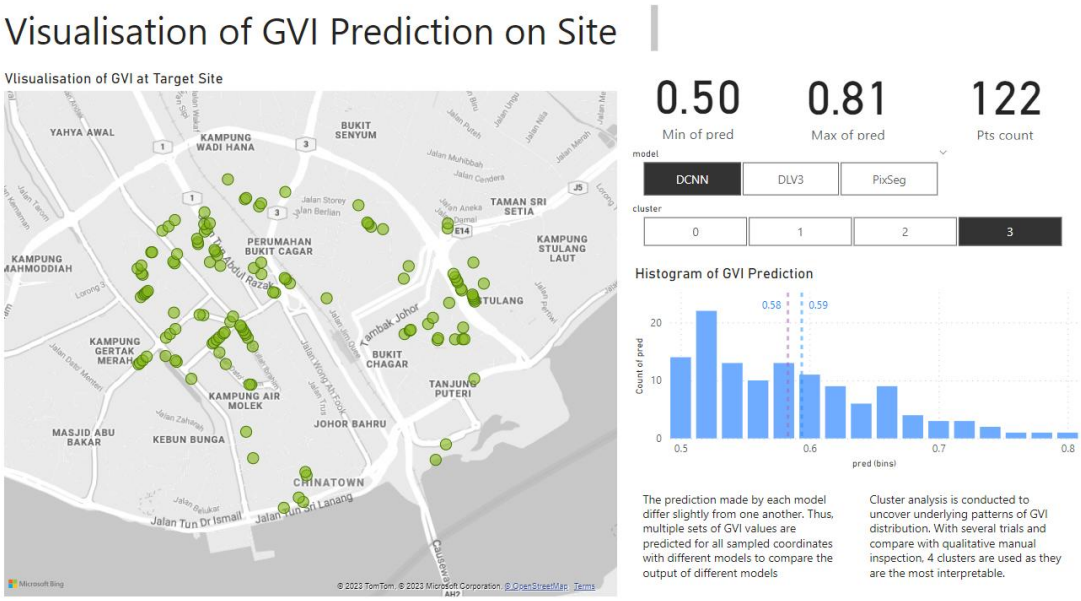

Figure 4.23 Visualization of Cluster 3 for DCNN Kmeans clustering.

Cluster 3 has the highest predicted GVI values. There are 122 spots where GVI is in the higher range of 0.50 and 0.81. Their average and median GVI are 0.59 and 0.58 respectively. From the map plot, we can notice Cluster 3 to have a very similar distribution pattern compared with Cluster 2 as shown in Figure 4.24.

Figure 4.24 Comparison of Cluster 3 (right) distribution compared with Cluster 2 (left).

Nonetheless, by manually inspecting the GSV images for Cluster 3, we can see that there is a differentiator between data points in Cluster 3 and Cluster 2. In Cluster 3, data points are mostly located at areas that have lower density, smaller roads and are less

developed. Figure 4.26 illustrates GSV samples of Cluster 3. An indication of where images in Figure 4.26 are sampled from is displayed in map-plot in Figure 4.25.

Figure 4.25 Indication of the sampling location for GSV images displayed in Figure 4.26.

Figure 4.26 Sample GSV images marked in Figure 4.25.

4.3.5 Clustering Analysis Conclusion

In conclusion, the clustering analysis of the GVI values in Johor Bahru city center provides several key insights regarding the distribution of green views and urban design considerations:

Cluster 0 represents urban spaces with very low predicted GVI values. These spots are mainly located on highways and main roads without observable vegetation. The presence of

numerous low GVI spots in these areas highlights a fundamental flaw in vehicle-centric and careless urban planning that neglects the need of green spaces. It creates uncomfortable spaces for users and poses challenges for planting trees due to maintenance and arrangement issues.

Cluster 1 consists of spots with higher predicted GVI values compared to Cluster 0. These spots are more evenly scattered throughout the city center, particularly in active commercial and residential areas. These areas contribute significantly to the overall experience of urban space users. Cluster 1 spots exhibit a higher presence of green views, including green belts, street trees, and other forms of vegetation.

Cluster 2 includes spots with the second-highest predicted GVI values. They are primarily concentrated in the North, East, and West parts of the city center. Cluster 2 spots tend to be adjacent to green pocket spaces or belts, effectively permeating the city with greenery. These smaller green areas play a crucial role in enhancing the predicted GVI of the surrounding spots, offering green views in various locations. Incorporating more street trees in dense commercial areas, like the Chinatown street, has the potential to increase GVI despite limited space.

Cluster 3 represents spots with the highest predicted GVI values. Similar to Cluster 2, these spots are distributed in a comparable pattern, primarily in less dense and less developed areas with smaller roads. Although they share a distribution pattern with Cluster 2, the differentiating factor is the lower density and less developed nature of Cluster 3 areas. These spots offer a higher abundance of green views and contribute to a higher GVI.

Table 4.2 shows the mean GVI predictions and number of samples of each cluster for DCNN's GVI predictions. From the table, we can see that Cluster 0 and Cluster 1 is more predominant in the target site compared with that of Cluster 2 and 3. This shows that there are still many room of improvements to incorporate Green View in Johor Bahru city center.

Table 4.2 DCNN KMeans clusters with their respective mean GVI predictions.

Cluster	Number of Samples	Mean GVI Predictions
0	292	0.012675
1	310	0.171307
2	278	0.327357
3	122	0.501539

While some of the reasons behind the dominance of Cluster 0 and Cluster 1 are due to deep rooted urban planning issue that cannot be easily reversed such as too many highways and main roads, lack of green space incorporation in older streets, there are ways that we can do to optimize GVI values in target site based on the existing conditions. For instance, from Cluster 2, we realize that the inclusion of green belts, street trees and small green pocket areas, urban designers can significantly enhance the GVI values and overall urban experience for residents and visitors. This illustrates how important it is to develop effective methods for us to analyze green views in target site and develop appropriate solutions to improve GVI accordingly.

4.4 Dashboard

As part of this project, a comprehensive analysis was conducted to assess the distribution of green views within the Johor Bahru city center. The dashboard provides a user-friendly interface that allows stakeholders and urban planners to explore the distribution of Green View Index (GVI) values across the target site while inspecting the errors and bias underlying the prediction models. In the following figures, developed dashboards are presented and elaborated.

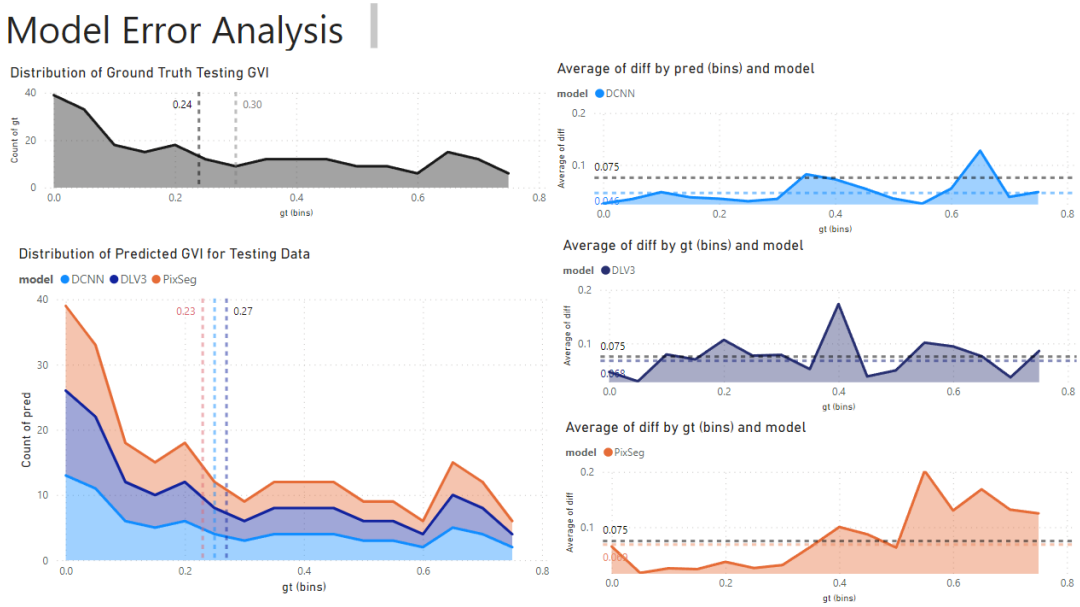

Figure 4.27 This dashboard investigates the error of each model at different predicted GVI values.

In the first chart on the top left corner, the distribution of ground truth GVI values for test data is plotted to be compared with GVI predictions of each model in the stacked chart below it. The 2 constant dotted lines in the ground truth GVI distribution chart represent median and mean respectively while the dotted lines in GVI prediction distribution chart represent the mean for each model prediction. With this, we can get a general idea of how the distribution of GVI predictions of each model compares with the ground truth.

On the other hand, the errors of each prediction model are studied with the charts on the right-hand side. The absolute error between GVI prediction and GVI ground truth is plotted against the GVI ground truth to investigate the errors for each model at different GVI

levels. These charts allow us to break down and analyze the accuracy of models at different situations, making the models more interpretable.

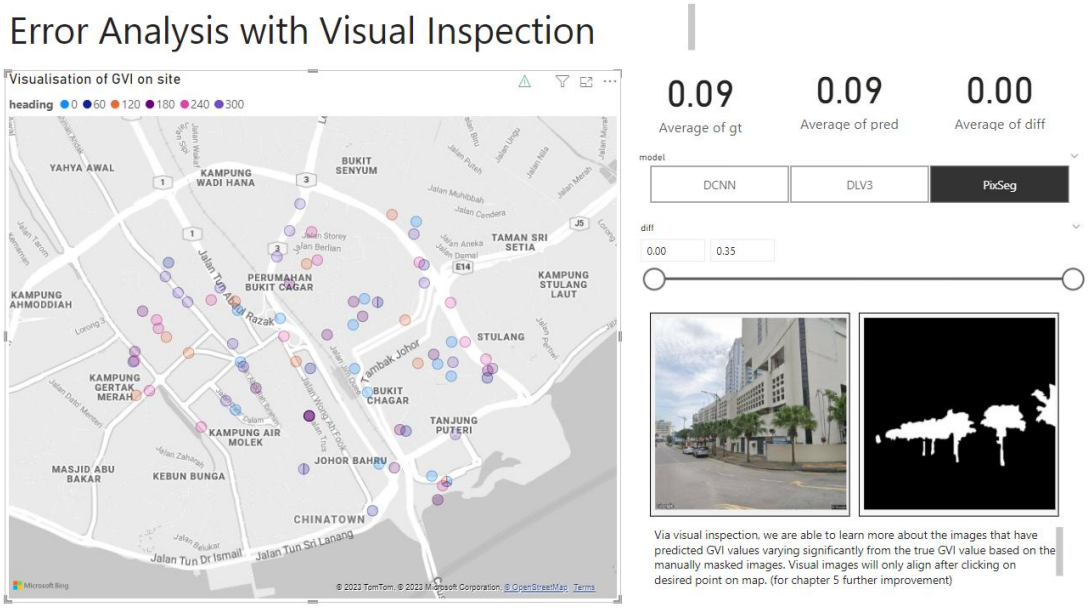

Figure 4.28 This dashboard visualizes the GSV image and label to allow more detailed error analysis of model with visual inspection.

Visual inspection of test data is another essential key for model development. By looking into the original GSV image and label data and comparing them with the predicted GVI, one can get a better idea about the possible reasons leading to error in prediction.

The map plot on the left visualizes the points and headings of GSV test data. By selecting or clicking on the point that we wish to inspect, we are able to view its respective GSV image and label and gauge the underlying problems leading to prediction error. The respective ground truth GVI, prediction and their difference are displayed on the cards.

To enable more flexibility in error inspection, two slicers are added to control the scope of data. For instance, if one wants to review the error larger than 0.20 in DCNN model predictions, one can adjust the slicer settings accordingly. This makes the work of inspection much more convenient as one is able to focus the scope of review to according to their needs.

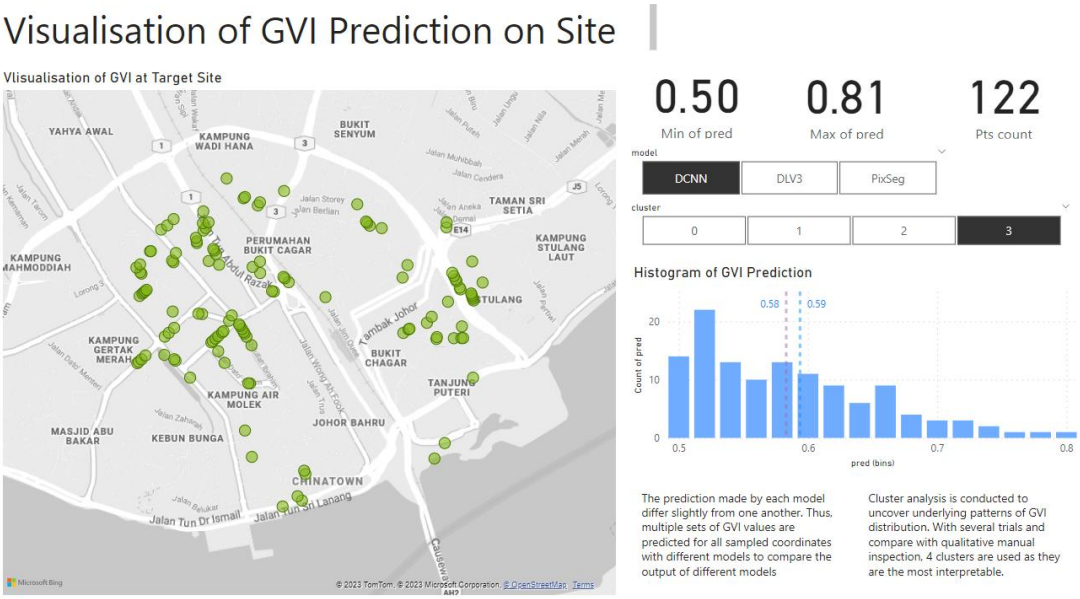

Figure 4.29 This dashboard visualizes the GVI predictions of all GSV data collected on site.

Through this dashboard, users can visualize the spatial distribution of the clusters on an interactive map. The map highlights the locations of spots within each cluster and provides insights into their respective GVI values. The greener a point is, the higher its GVI prediction; the redder a point, the lower its GVI prediction. On the right corner of the dashboard, the minimum and maximum GVI prediction, along with the number of point locations are visualized to provide a basic idea of the GVI predictions of the visualized data points. From the histogram, we can also observe the distribution of predicted GVI values for the visualized data.

The slicers are established based on “models” and “cluster”, with the former enabling us to visualize the predictions based on different models and the latter being used to carry out clustering analysis.

4.5 Chapter Summary

In conclusion, among DCNN, DeepLabV3+ and Pixel Segmentation models trained to predict GVI, DCNN has the greatest performance in terms of accuracy and robustness with. In terms of inference time, DCNN has a moderate inference time of 43.87s for 1000

predictions, which is in between 9.99s and 121.83s for Pixel Segmentation model and DeepLabV3+ respectively. Therefore, DCNN is deemed to have the best overall performance.

For clustering analysis, with experimentation on various clustering approaches, we find out that Kmeans with 4 clusters is the most suitable clustering approach for the GVI prediction in Johor Bahru city center. By applying this clustering approach on the DCNN GVI predictions, we can notice patterns in GVI distribution in target site. For instance, Cluster 0 with low GVI predictions are mainly focused on highways and the South part of the site with highly dense commercial buildings; Cluster 1 with moderately low GVI are the most evenly scattered cluster across the site; Cluster 2 with second highest GVI predictions are usually adjacent to green pocket spaces and belts; Cluster 3 with the highest GVI predictions are located in the less developed areas within the city center.

By carrying out clustering analysis, one can understand the underlying patterns that affect how much the people in the city makes experience greens in their daily lives and thereby generate appropriate solutions accordingly to optimize GVI and improve urban spatial experience in the target site.